Finite Element Model of a complex Glass Forming Process as a Tool for Control Optimization

Felix Sawo* and Thomas Bernard
Fraunhofer Institute for Information and Data Processing IITB,
*Corresponding author: Fraunhoferstr. 1, 76131 Karlsruhe, Germany, Felix.Sawo@iitb.fraunhofer.de

Abstract: This paper addresses the modeling of a complex glass forming process as an example of a complex, nonlinear distributed parameter system. The system is modeled by a fluid dynamics approach, which means that the forming is regarded as a fluid with free surfaces. Here, the coupling of the forming process with the heat flow is considered. The influence of crucial model parameters (e.g., dynamic viscosity) to the shape of the glass tube and the dynamic behavior is investigated by means of simulation results.

1 Introduction

In a wide variety of industrial processes the underlying physical phenomenon has to be regarded as spatially distributed. Examples are rheological forming processes in industrial glass furnaces where heat conduction, radiation, and fluid dynamics are the main physical effects. In the manufacture of optical fibers, the precise control of the diameter is critical to the final performance of the product. It is of significant interest to quantify the effects that cause changes in the diameter.

For investigating, controlling, and optimizing such industrial processes, simulation models have become increasingly important over the last few decades. The model would be very helpful for following problems that are particularly associated with the production of quartz glass tubes: **(1)** investigation of ovality and siding, **(2)** optimization of process and construction parameters (e.g., design of temperature profile of the furnace), **(3)** investigation of the influence of disturbances, and **(4)** design and optimization of process control strategies. The variation of only one parameter is nearly impossible for an *experiment based* investigation, since many parameters naturally vary in each production. The possibility to study the influence of single parameters is the great advantage of a *simulation based* approach.

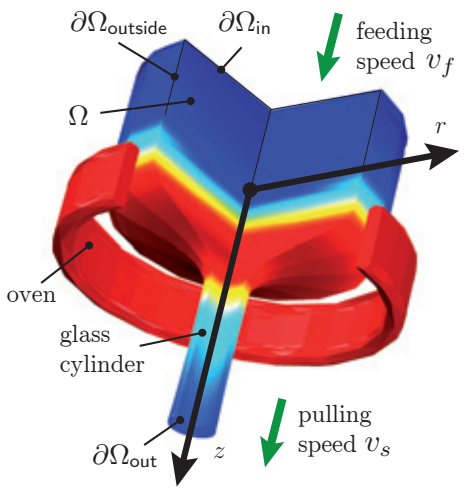

Figure 1: Setup of the glass forming process.

The glass forming process is modeled by a fluid dynamics approach, which means that the forming is regarded as fluid with free surfaces [5, 6, 7, 8]. The model can be simplified by the assumptions of axisymmetric and thin layer flow, i.e., wall thickness is much smaller than the length of the forming zone. This leads to the so-called *Trouton model* [6].

The main problem of correctly modeling glass forming processes is the tremendous distortion during the forming process. The existing process models may be classified into two groups [4]. The *interface-tracking techniques* are based on updating the underlying mesh as the glass flow evolves in order to track the interface [9]. The main technique is the arbitrary Lagrangian–Eulerian description that is considered in this paper. The *interface-capturing techniques* are based on both a flow equation and advection equation governing the time-evolution of an interface function [4], such as the level set methods [2]. The objective of this paper is to extend and further develop our finite element model [1] to be used for industrial purposes.

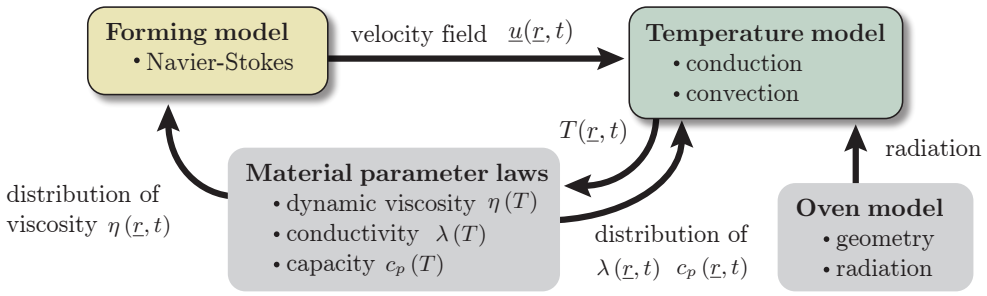

Figure 2: Components of the entire rheological forming model and their coupling terms.

2 Rheological Forming Model

The industrial process that is considered in this paper is a complex rheological forming process producing thin glass tubes from thick cylinders. The main physical phenomena arise from *radiation*, *heat conduction*, and *fluid dynamics*. These industrial processes are strongly nonlinear in particular due to the impact of radiation and nonlinear material parameter laws. In addition, the forming process involves a wide temperature range and is characterized by large deformations.

The process setup is visualized in Figure 1. The cylinder is fed with slow velocity v_f in an oven where it is heated up to its forming temperature. Below the oven the tube is pulled with a higher velocity v_s resulting in thin glass tubes. The geometry of the resulting tubes strongly depends on the velocities v_f and v_s, and the oven temperature T_{oven}.

In this section, we present the components of the mathematical model that can be used to describe glass forming in general. This involves solving the motion of the glass, the heat flow, and nonlinear material laws. The individual components of the model and their coupling terms are visualized in Figure 2.

2.1 Forming and temperature model

In general, the state that uniquely describes the complex rheological forming process does not only depend on time but also on the spatial coördinate $\underline{r}$. The corresponding equations are derived using a fluid dynamic approach, i.e., the forming is regarded as a Newtonian fluid with free surfaces. Basically, the model consists of two main parts describing **(a)** glass motion and **(b)** heat flow in the glass.

The main goal is the accurate calculation of *velocity field* $\underline{u}(\underline{r},t) : \mathbb{R}^2 \times \mathbb{R} \to \mathbb{R}^2$, *pressure distribution* $p(\underline{r},t) : \mathbb{R}^2 \times \mathbb{R} \to \mathbb{R}$ and *temperature distribution* $T(\cdot)$ inside the fluid, i.e., in the solution domain $\Omega \in \mathbb{R}^2$. In three-dimensional space this yields a complex model with high computational effort. For some assumptions, a simpler flow model can be developed. Here, the process is considered to be axisymmetric, e.g., the spatial coördinate $\underline{r} := [r,z]^{\mathrm{T}} \in \mathbb{R}^2$ consists of radius r and height z. The coördinate frame characterizing the forming process is depicted in Figure 1.

Incompressible Navier–Stokes Equation
For the actual motion of the rheological material, the governing equations are as follows

$$\begin{aligned} \rho\frac{\partial \underline{u}}{\partial t} &= \nabla \underbrace{\left[-pI + \eta\left(\nabla\underline{u} + (\nabla\underline{u})^T\right)\right]}_{=:\sigma} + \ldots \\ &\quad -\rho\,(\underline{u}\cdot\nabla)\,\underline{u} - \rho\,\underline{g}\ , \\ \nabla\underline{u} &= 0\ . \end{aligned} \tag{1}$$

The first equation is the momentum balance; the second one is simply the equation of continuity for incompressible fluids. The *density* of the considered material is denoted as ρ and the *dynamic viscosity* is represented by η.

For the considered forming process, conditions are specified on the boundaries where the fluid is supposed to enter the domain Ω. The first is to set the velocities equal to given vectors

$$\begin{aligned} \underline{u} &= \underline{u}_{\mathsf{in}} \quad \text{for} \quad \underline{r} \in \partial\Omega_{\mathsf{in}}\ , \\ \underline{u} &= \underline{u}_{\mathsf{out}} \quad \text{for} \quad \underline{r} \in \partial\Omega_{\mathsf{out}}\ . \end{aligned}$$

The condition at the boundary $\partial\Omega_{\mathsf{outside}}$ is specified as a so-called *open boundary*. This implies that the total stress in tangential direction is equal to zero.

Since the material parameters strongly depend on the temperature, a model for the *temperature distribution* $T(\underline{r},t)$ in the glass tube is required; described in the following.

Heat Transfer Equation

The heat flow in glass tubes can be described by the energy equation for incompressible fluids as follows

$$\rho c_p \frac{\partial T}{\partial t} = \underbrace{\nabla \cdot (\lambda \nabla T)}_{\text{heat conduction}} - \underbrace{\rho c_p \, \underline{u} \cdot \nabla T}_{\text{convection term}} \quad , \qquad (2)$$

where c_p denotes the *heat capacity* at constant pressure and λ the *thermal conductivity*. The convection term is characterized by the *velocity field* $\underline{u}(\underline{r},t)$, which needs to be derived by the aforementioned Navier–Stokes equation.

The source driving the heating process is restricted to *radiation heat transfer*. This is imposed as a *boundary condition* by setting the gradient of temperature at the boundary $\partial\Omega_{\text{outside}}$ as follows

$$\underline{n} \cdot (\lambda \Delta T) = \epsilon\sigma \left(T_{oven}^4 - T^4\right) \quad \text{for } \underline{r} \in \partial\Omega_{\text{outside}} \ .$$

Here, $\underline{n}$ represents the inward normal vector, ϵ is the surface emissivity, and σ is the Stefan-Boltzmann constant. For practical applications, the so-called *oven model* needs to be identified as precise as possible. Basically, this model defines the profile of the oven temperature T_{oven} that strongly depends on the geometry of the heating tube.

2.2 Nonlinear material parameter laws

The material parameters characterizing the forming process vary strongly with the relevant temperature range from 20 ℃ up to more than 2000 ℃. Temperature variations within this range cause significant changes in the mechanical properties of the glass. Thus, tremendous nonlinearities are introduced into the forming model (1) and temperature model (2). In the following, the nonlinear material parameter laws are described in more detail.

Dynamic Viscosity Model

In general, the *dynamic viscosity* η represents the fluids resistance to the flow. In the case of glass, the viscosity strongly depends on the temperature and the range for varying temperature is relatively large. It increases rapidly as a glass melt is cooled, so that its shape will be retained after the forming process.

Typically the temperature dependance for the viscosity of glass is given by the Vogel-Fulcher-Tammann (VFT) relation. However, in order to consider a more extended temperature range, the following *modified relation* can be deduced

$$\log(\eta) = \eta_{\text{min}} + \frac{1}{2}(\eta_{\text{max}} - \eta_{\text{min}})(\tanh(c_1 T + c_2) + 1) \quad , \qquad (3)$$

where η_{min}, η_{max}, c_1, and c_2 represent model parameters to be identified. Figure 3 visualizes the viscosity η versus temperature T for certain model parameters. It is obvious that the minimum and maximum of the viscosity is respectively respresented by η_{min} and η_{max}, whereas c_1 and c_2 characterize the actual shape of the gradient.

Conductivity and Heat Capacity

In general, the *conductivity* and *heat capacity* characterize the heat transfer through the rheological material. The parameters depend on the actual temperature; although the nonlinearity is less tremendous as it is for the viscosity. Here, the following equations are used

$$\begin{aligned} \text{conductivity} \quad & \lambda = k_\lambda^1 + k_\lambda^2 \, T^3 \\ \text{heat capacity} \quad & c_p = k_c^1 + k_c^2 \left(T - k_c^3\right) \end{aligned}$$

where k_λ^1, k_λ^2, k_c^1, and k_c^1 denote model parameters to be identified.

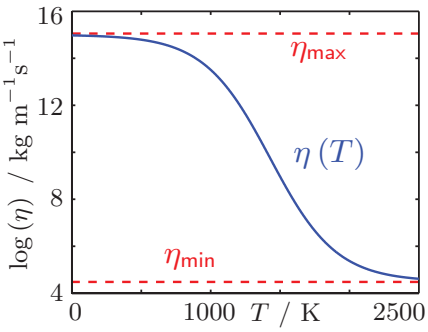

Figure 3: Dynamic viscosity η vs. temperature T.

2.3 Deformed mesh

The numerical simulation of the considered rheological forming process requires coping with strong distortions of the continuum. In the continuum mechanics there are *two classical descriptions* of motion: **(a)** the Lagrangian and **(b)** the Eulerian description. The pure *Lagrangian description* is an approach where the mesh moves with the material. This allows an easy tracking of surfaces; however is restricted to relatively small displacements. When the material motion is more complicated, such as in the case of fluid flow problems, the *Eulerian description* can be used. For such descriptions the mesh remains fixed while the material passes through it. The *arbitrary Lagrangian–Eulerian* description (ALE) was developed in an attempt to combine the advantages of aforementioned classical descriptions; their drawbacks were minimized as far as possible [3, 9, 10]. It allows the boundaries to move without the need for the mesh to follow the material. Here, the ALE method is used for simulating the forming process.

Free Surface Model
In order to follow the glass motion, the motion of the moving mesh needs to be coupled to the motion normal to the surface. Therefore, the boundary condition for the mesh equations on the free surface $\partial\Omega_{\text{outside}}$ is given by

$$(x_t, y_t)^T \cdot \underline{n} = \underline{u} \cdot \underline{n} \ ,$$

where $(x_t, y_t)^T$ is the velocity of the moving mesh and $\underline{n}$ the boundary normal. In Figure 4, the deformation of an initial mesh using the ALE technique is visualized for a rough mesh. It is obvious that the boundary $\partial\Omega_{\text{outside}}$ follows the glass motion $\underline{u}(\underline{r}, t)$ without the mesh getting distorted.

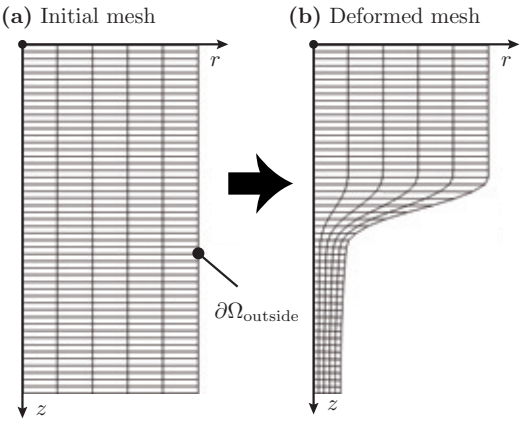

Figure 4: Arbitrary Lagrangian–Euler mesh.

3 Simulation Results

In order to get an impression of the system behavior of this complex, highly coupled, and nonlinear process some characteristic stationary and time dependent results are presented in this section. In particular, the influence of single parameters in the viscosity model (3) to the shape of the glass tube is investigated.

The *initial/boundary conditions* for the pulling speed, feeding speed, and oven temperature are assumed to be as follows:

pulling speed	$v_{f0} = 0.2\,\text{mm/s}$
feeding speed	$v_{s0} = 2.0\,\text{mm/s}$
oven temperature	$T_{\text{oven}} = 2300\,^{\circ}C$

The temperature distribution and glass shape that results from aforementioned conditions is visualized in Figure 5 **(a)**.

3.1 Time dependent results

For investigating the dynamics of the forming process a step response with respect to the manipulated variable pulling speed $v_s = 2 \Rightarrow 1\text{mm/s}$ has been performed. In Figure 5, the response of the temperature distribution and the glass tube shape is depicted for different time steps $t \in \{0, 500, 1000, 2000\}\,\text{s}$. It is obvious that the step with respect to the pulling speed v_s causes a change in the diameter D below the heating tube. Due to the coupling of the forming model (1) with the temperature model (2), the increasing diameter respectively yields a change of the temperature distribution inside the glass tube.

3.2 Variations in the viscosity model

A crucial parameter for the behavior of the forming process is the dynamic viscosity η, and especially its dependency on the temperature T. Here, the response to a step in pulling speed v_s is investigated for different assumed viscosity models. To be more specific, the minimum viscosity $\eta_{\min}$ and the maximum viscosity $\eta_{\max}$ was varied as follows

$$\eta_{\min} \in \{4.7, 4.9, \ldots, 5.9\}$$
$$\eta_{\max} \in \{13.7, 13.9, \ldots, 14.9\}$$

The resulting set of viscosity models is visualized in Figure 6/7 **(a)**. The sensor position for "measuring" the diameter D has been placed at height $z = -0.2\,\text{m}$ in the simulation which is close to the real position. Figure 6/7 **(b)** shows the response of the diameter D below the heating for different assumed viscosity models. It is obvious that the shape of the viscosity model $\eta(T)$ has a strong influence on the process dynamics. Roughly speaking, for lower viscosity the dynamic slightly increases and the overshooting decreases. The influence of the dynamic viscosity η on the glass shape and the velocity inside the glass is depicted in Figure 6/7 **(c)**–**(d)**.

4 Conclusion and Future Work

In this paper, we have demonstrated the feasibility of simulating glass forming processes by means of a *fluid dynamics approach*. The main components consists of a *forming model* and a *temperature model*. Compared to our previous research work the coupling between these two components were considered during the simulation. By this means, the temperature distribution and deformation of glass tubes can be predicted throughout the furnace.

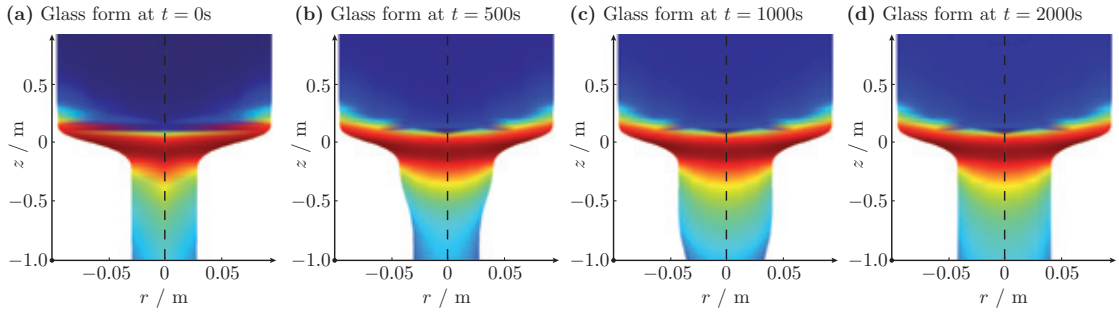

Figure 5: Response of temperature profile and glass tube shape to a step in pulling speed $v_s = 2 \Rightarrow 1$mm/s for different time steps: **(a)** $t = 0$ s, **(b)** $t = 500$ s, **(c)** $t = 1000$ s, and **(d)** $t = 2000$ s.

The model can be used to investigate the influence of single parameters to the dynamic behavior of the forming process. In this paper, the influence of the *viscosity model* to the *glass shape* was particularly investigated. It turned out that the viscosity is a crucial parameter that need to be accurately identified for obtaining a precise model.

Future work is devoted to the investigation of further parameters in terms of a sensitivity analysis. In addition, the model parameters need to be identified for a given forming process, so that the model can be used for designing control strategies and optimizing the forming process.

References

[1] T. Bernard and E. Ebrahimi Moghaddam, *Nonlinear Model Predictive Control of a Glass forming Process based on a Finite Element Model*, Conference on Control Applications (CCA 2006) (Munich, Germany), October 2006.

[2] W. Dijkstra and R. M. M. Mattheij, *Numerical Modelling of the Blowing Phase in the Production of Glass Containers*, Electronic Journal of Boundary Elements **6** (2008), 1–23.

[3] J. Donea, Antonio Huerta, J.-Ph. Ponthot, and A. Rodrguez-Ferran, *Encyclopedia of Computational Mechanics*, ch. Arbitrary Lagrangian – Eulerian Methods, 2004.

[4] C. G. Giannopapa, *Level-set Method used to Track the Glass-Air Interface in the Blow Step of Glass Containers*, ASME J. Manuf. Sci. Eng. (2007).

[5] P. D. Howell, *Extensional Thin Layer Flows*, Ph.D. thesis, St. Catherine's College, Oxford, 1994.

[6] D. Krause, *Mathematical Simulation in Glass Technology*, Springer, 2002.

[7] A. Mawardi and R. Pitchumani, *Numerical Simulations of an Optical Fiber Drawing Process Under Uncertainty*, Journal of Lightwave Technology **26** (2008), 580–587.

[8] M. R. Myers, *A Model for Unsteady Analysis of Preform Drawing*, AIChE Journal **35** (1989), no. 4, 592–602.

[9] M. Souli, A. Ouahsine, and L. Lewin, *ALE Formulation for Fluid-Structure Interaction Problems*, Comput. Methods Appl. Mech. Engrg. **190** (2000), 659–675.

[10] A. Weddemann and V. Thümmler, *Stability Analysis of ALE-Methods for Advection-Diffusion Problems*, COMSOL Conference (Hannover), 2008.

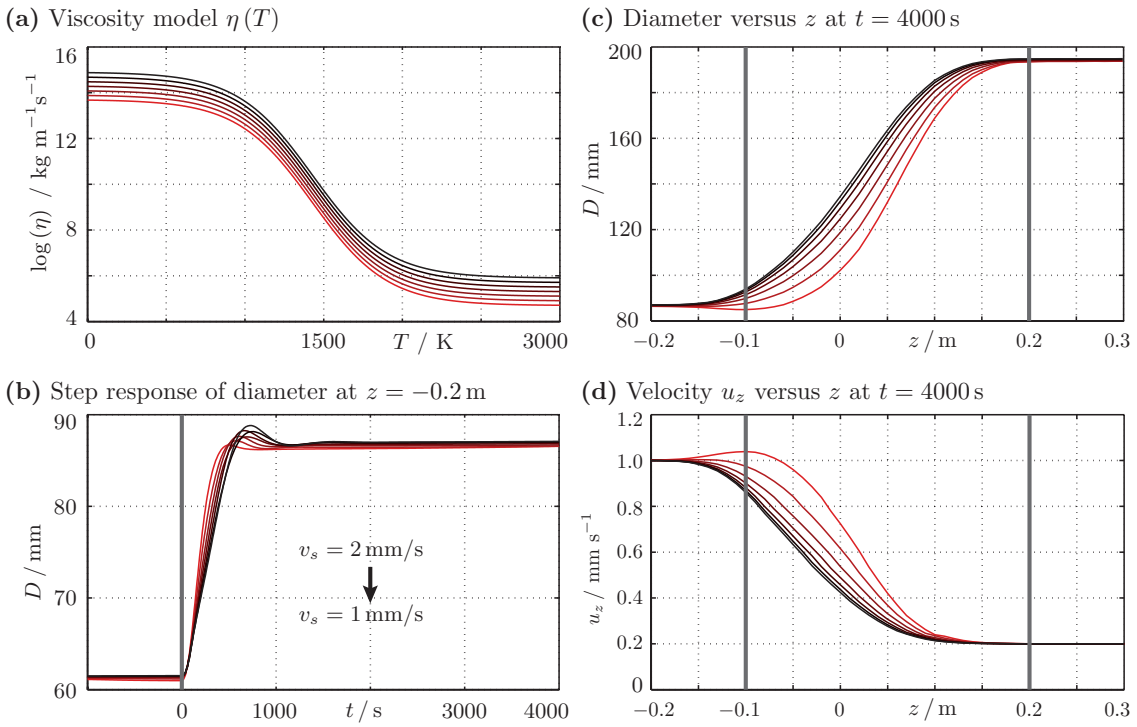

Figure 6: Simulation results for various viscosity models. **(a)** Set of viscosity models $\eta(T)$ used for the simulation. **(b)** Response of diameter D to step in pulling speed $v_s = 2 \Rightarrow 1\mathrm{mm/s}$. Stationary profile of **(c)** tube geometry and **(d)** velocity u_z for different viscosity models.

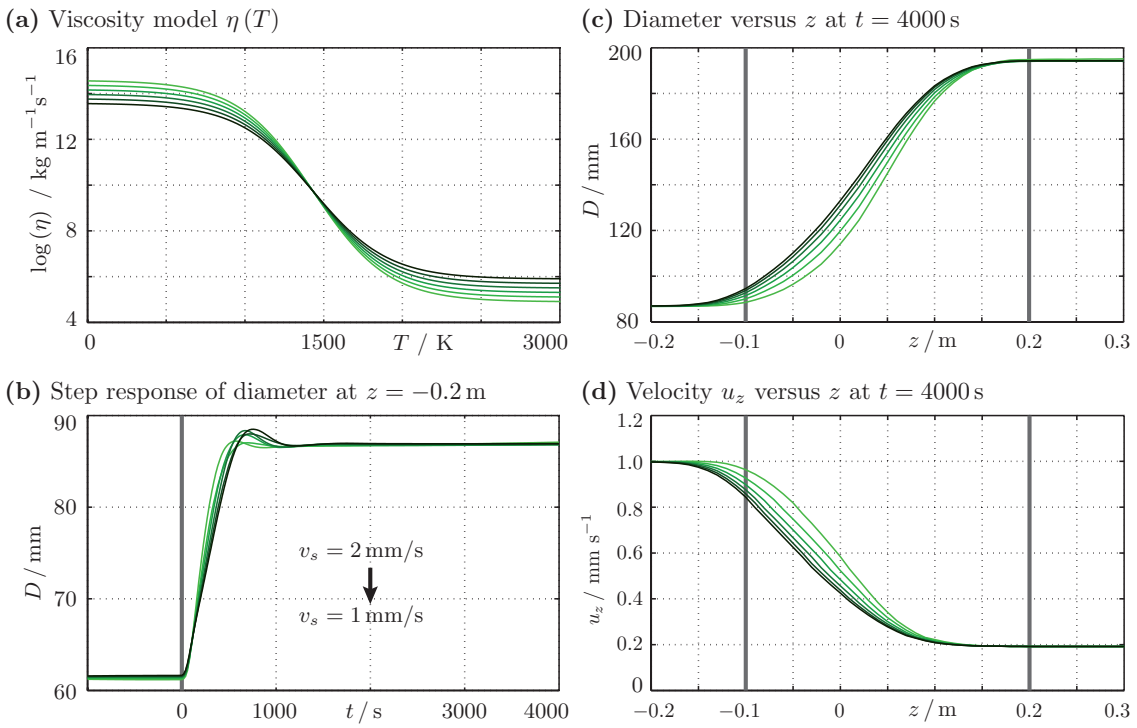

Figure 7: Simulation results for various viscosity models. **(a)** Set of viscosity models $\eta(T)$ used for the simulation. **(b)** Response of diameter D to step in pulling speed $v_s = 2 \Rightarrow 1\mathrm{mm/s}$. Stationary profile of **(c)** tube geometry and **(d)** velocity u_z for different viscosity models.